Proceedings of the American Control Conference
San Diego, California • June 1999

Trajectory Morphing Applied to Epitaxial Thin Film Growth

A. P. Engelmann, David G. Meyer*, and John Hauser
Nonlinear and Real-Time Control Laboratory
Dept. of Electrical and Computer Engineering
University of Colorado, Boulder, CO 80309-0425
engelman@wonko.colorado.edu dgm2r@wonko.colorado.edu hauser@talon.colorado.edu

Russell Caflisch
Mathematics Department
University of California
Los Angeles, CA 90095-1555
caflisch@math.ucla.edu

Abstract

This paper presents results showing that trajectory morphing may be used to explore the trajectory space of an epitaxial thin film growth system.

1 Introduction

Epitaxial thin film growth occurs when a thin film is constructed in a layer by layer fashion. One example of such a method is Molecular Beam Epitaxy (MBE). In MBE, thin film material (e.g. semiconductor material) is heated in a crucible which resides in a vacuum chamber. The heated material evaporates, exits the crucible, and lands on a substrate. A thin film grows on the substrate in a layer by layer manner. Control of epitaxial thin film growth has consisted mostly of simple single-loop feedback of operating variables. For example, PID (proportional integral derivative) regulation of effusion cell crucible temperature and flux [10] [8], and subtrate temperature [1]. No attempt at directly regulating critical crystal properties has been made.

Operators wishing to grow a semiconductor crystal have relied on their own expertise and experience to schedule setpoints of incident flux (crucible temperature) and substrate temperature. The setpoints are regulated with PID control. As desired growths become more complicated, there is naturally a need to more directly regulate crystal properties.

Several recent developments have made it possible to begin exploring in formal ways the trajectory space of epitaxial growth during MBE. First, an ODE (ordinary differential equation)model has been developed which captures features of multi-layer epitaxial growth [4] during MBE. Other PDE (partial differential equation) models have been developed [2] [3] , but the new model allows application of control theory for systems described by ODE's. The ODE model includes important growth phenomena such as island growth and coalescence. Additionally, a model output, the step edge density, closely correlates with an actual sensor signal, RHEED (Reflection High-Energy Electron Diffraction). Second, a new method for exploring the trajectory space of a nonlinear system has been developed, **trajectory morphing** [6]. Trajectory morphing employs a simplified system model to come up with a desirable approximate trajectory; then projection and homotopy is used to "morph" the desirable approximate trajectory into a desirable true trajectory for the full model. It is emphasized here that the result of trajectory morphing is a nominal (open loop) trajectory that is "close" to a desirable trajectory. Of course, in implementation, one would attemp to stabilize the open loop trajectory with feedback.

This paper presents results on applying trajectory morphing to epitaxial thin film growth as modeled by [4]. Section 2 outlines the growth model. We have derived a simplified growth model, suitable for use in morphing, and this is also presented. The fundamentals of trajectory morphing are reviewed in Section 3. Section 4 presents results from a simulation study applying trajectory morphing to the thin film growth system.

2 Multi-Layer Epitaxial Growth Model

This section presents an overview of the *Multi-Layer Epitaxial Growth Model* (MLEGM) [4] for thin films. Each layer of the thin film is modeled as one atom thick. Atoms on each layer that are grouped with other atoms form an island. Atoms that are not attached to an island are free and are called adatoms. The model contains three states for each layer of growth simulated. The states for the k^{th} layer are ρ_k, the adatom density (adatoms per unit area); ψ_k, the coverage (area coverage by islands); and n_k, the island density (average

*Corresponding author. Research supported in part by the National Science Foundation under DMS-96158-54, by the National Institute of Standards under contract number 50SBNBC8517, and by the Defense Advanced Research Projects Agency under contract numbers MDA972-93-H-0005 and MDA972-95-1-0016.

number of islands per unit area). The ρ_k and ψ_k states are normalized to the number of atoms per lattice site so their maximum values are one. The model assumes that adatoms move by standard diffusive lattice-site hopping; when two come together they bond into an island. As other adatoms diffuse to an island, they attach and consequently the island grows. Atoms on top of an island are considered to be on the next layer. The diffusive mobility of an island is taken to be zero.

The differential equations describing how the states change are:

$$\begin{aligned} \frac{d}{dt}(\rho_k(\psi_{k-1}-\psi_k)) &= J(\psi_{k-1}-\psi_k) - q_k f_k^- \\ &\quad -q_{k-1}f_{k-1}^+ - 2m_k \\ \frac{d}{dt}\psi_k &= q_k v_k + 2m_k \\ \frac{d}{dt}n_k &= m_k - c_k \end{aligned} \tag{1}$$

with constitutive equations:

$$\begin{aligned} q_k &= \sqrt{\psi_k n_k} \\ v_k &= f_k^- + f_k^+ \\ f_k^+ &= D_+\rho_{k+1}(\tfrac{1}{r_{k+1}} + \tfrac{1}{b_k})(\psi_k - \psi_{k-1}) \\ f_k^- &= D_-\rho_k(\tfrac{1}{r_k} + \tfrac{1}{b_k})(\psi_{k-1} - \psi_k) \\ m_k &= D_0(\psi_{k-1}-\psi_k)\rho_k^2 \\ c_k &= 2v_k n_k / r_k \\ b_k &= \sqrt{\psi_k / n_k} \\ r_k &= b_k(\sqrt{\psi_{k-1}/\psi_k} - 1) \end{aligned} \tag{2}$$

Terms in (1), with respect to the k^{th} layer, are: q_k the island step edge density, v_k the island step edge velocity, f_k^+ the adatom flux (up flow) from the k layer to the $k+1$ layer, f_k^- the adatom flux (down flow) from the k layer to the $k-1$ layer, m_k the nucleation rate of new islands and c_k the coalescence rate of islands. Also, b_k is the average island diameter and r_k is the average inter-island distance.

The first differential equation in (1) expresses mass conservation: Adatoms arriving on the k^{th} layer must either jump up, down, nucleate, or add to ρ_k. The second equation in (1) equates the rate of change of layer coverage to the sum of a nucleation contribution and growth by attachment (advancing step edges at velocity v_k). The last equation simply says the rate of change of island number density is the difference between nucleation and coalescence. The constitutive relations in (2) are more difficult to concisely explain. A full length paper on the model is presently being prepared.

The control variables are J, the incident adatom flux, and D_0, the diffusive mobility coefficient which is physically controlled by adjusting the substrate temperature. The terms D_+ and D_- refer to different diffusion coefficients for the upward and downward flux of adatoms since diffusion at a step edge can be distinct from diffusion along a terrace. For simplicity we took $D_0 = D_- = D_+ = D$, though this is not necessary for the methods to work. The model output is $q = \sum_{k=1}^{N} q_k$ where N is the number of layers. As mentioned, this output corresponds well to an actual RHEED sensor signal.

Figure 1 shows model states and output for a four layer simulated growth. The inputs were $J = 1/4, D = 25 \times 10^3$ resulting in $D/J = 10^5$, which is characteristic of MBE. The output, q, exhibits characteristic oscillatory behavior. The coverage states, ψ_k, are monotonically increasing and show good layer-by-layer growth. The island densities n_k, small at layer start, are maximum near the middle of the layer's growth then drop off to zero at layer end. It is noted that all of the states have positive values. A negative adatom density, coverage, or island density is clearly not physical.

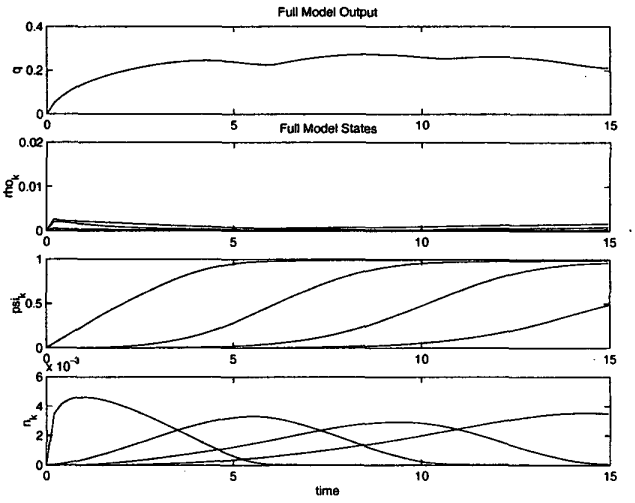

Figure 1: Full Model Output and States for Constant Controls

The interested reader is referred to [4] for full details on the derivation of the model.

2.1 Simplified Model

To apply trajectory morphing, one needs a simple model of the system to be morphed. The need for the simple model is reviewed in Section 3. The full MLEGM model presented in the previous section is highly coupled and nonlinear. It is non-obvious how to cooperatively use J and D to steer the system in a specified manner. We had hoped to find a physically plausible simplified model that was also differentially flat so as to make the generation of approximate trajectories rather trivial. Unfortunately, we could not accomplish that. Instead, simulation and order of magnitude analysis were used to eliminate terms, and develop approximations, in the MLEGM.

The following approximations of (2) were made:

$$\begin{aligned} f^+_{k\_0} &= D_+\rho_{k+1}(\tfrac{1}{r_{k+1}}+1)(\psi_k-\psi_{k-1}) \\ f^-_{0k} &= D_-\rho_k(\tfrac{1}{r_k}+1)(\psi_{k-1}-\psi_k) \\ v_{0k} &= f^-_{0k}+f^+_{0k-1} \\ m_{0k} &= 0.01D_0(\psi_{k-1}-\psi_k)\rho_k \\ c_{0k} &= 2v_{0k}n_k/r_k \end{aligned} \tag{3}$$

where the 0 subscript denotes terms for the simple model. Figure 2 shows the output and states for the simple model with $J = 1/4$, $D = 25\times10^3$. Comparing Figures 1

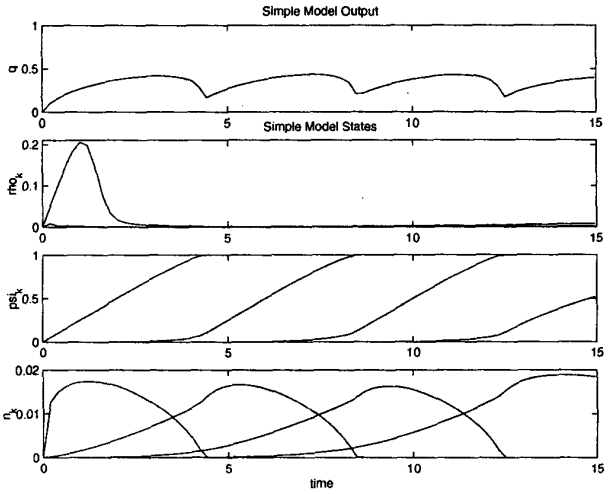

Figure 2: Simple Model Output and States for Constant Controls

and 2 reveals that, while their are inevitable quantitative differences, the simplified model behaves in manner qualitatively similar to the MLEGM. This is important.

3 Trajectory Morphing

Trajectory morphing [6] is a method for exploring the trajectory space of a nonlinear system. Trajectories of a nonlinear system can be defined as follows. Let f be a $C^r, r \geq 1$, mapping from $\mathbb{R}^n \times \mathbb{R}^m$ to $\mathbb{R}^n$ and consider

$$\Sigma: \quad \dot{x}(t) = f(x(t), u(t)), \quad x(0) = x_0 \tag{4}$$

Let $\mathcal{X}$ and $\mathcal{U}$ be the space of measureable functions from $\mathbb{R}^+$ to $\mathbb{R}^n$ and $\mathbb{R}^m$ respectively. A curve $(x(\cdot), u(\cdot)) \in \mathcal{X} \times \mathcal{U}$ satisfying 4 is a *trajectory* of Σ. Recent work has shown that the set of exponentially stabilizable trajectories has a manifold structure [7].

Trajectory morphing uses projection and homotopy as tools to explore the trajectory space. Consider the trajectory tracking projection operator $\mathcal{P} : (\alpha(\cdot), \mu(\cdot)) \mapsto (x(\cdot), u(\cdot))$ defined by

$$\begin{aligned} u(t) &= \beta(t, x(t), \alpha(t), \mu(t)) \\ \dot{x}(t) &= f(x(t), u(t)) \\ x(0) &= \alpha(0) \end{aligned} \tag{5}$$

where the feedback law β satisfies the invariance condition

$$\beta(t, \alpha, \alpha, \mu) = \mu \tag{6}$$

for any $(\alpha, \mu) \in \mathbb{R}^{n\times m}$ and $\forall t$. It is shown in [6] that $\mathcal{P}$ takes curves in an L_∞ neighborhood of $(\alpha(\cdot), \mu(\cdot))$ into system trajectories, i.e. it is a projection from the vector space of $(\alpha(\cdot), \mu(\cdot))$ curves onto the manifold of system trajectories.

Consider the optimization problem

$$\min_{(x(\cdot),u(\cdot))} \frac{1}{2} \|\mathcal{P}_\lambda(\alpha(\cdot), \mu(\cdot)) - (x_0(\cdot), u_0(\cdot))\|_2^2 \tag{7}$$

where $\mathcal{P}_\lambda : (\alpha(\cdot), \mu(\cdot)) \mapsto (x(\cdot), u(\cdot))$ is the trajectory tracking projection operator defined by

$$\begin{aligned} u(t) &= \beta(t, x(t), \alpha(t), \mu(t)) \\ \dot{x}(t) &= (1-\lambda)f_0(x(t), u(t)) + \lambda f(x(t), u(t)) \\ x(0) &= \alpha(0) \end{aligned} \tag{8}$$

where f_0 is the simple model, f is the full model and λ is a homotopy scalar that takes values from 0 to 1. The optimization problem above minimizes the tracking error between a desired trajectory of the simple system and a trajectory projected onto the system scaled by the homotopy factor λ. Once the minimization is complete, λ can be increased and the minimization performed again resulting in a trajectory that is closer to the full system trajectories. This process can be repeated until a minimization is found between the nominal trajectory and full system trajectories ($\lambda = 1$). In summary, the process is:

1. Design feedback law β that stabilizes (x_0, u_0) for f_0.
2. Increment λ and solve (7) using (x_0, u_0) as initial guess. Call solution (x_λ, u_λ).
3. Simulate f_λ to make sure β stabilizes (x_λ, u_λ). If not, redesign β.
4. Increment λ and solve (7) using (x_λ, u_λ) as an initial guess.
5. If $\lambda = 1$ stop; otherwise goto number 3.

3.1 Design of Stabilizing Feedback

Morphing requires a feedback[1] which exponentially stabilizes approximate trajectories. To this end, we designed a controller using Linear Quadratic Regulator

[1] A single feedback through all values of λ is not required, i.e., you can redesign the feedback at each step of the morphing process.

(LQR) theory (see [9]). The linearization of (1) along a desired trajectory (x^*, u^*) results in the linear time varying system

$$\dot{z}(t) = A(t)z(t) + B(t)v(t) \tag{9}$$

where $A(t) = D_1 f(x^*, u^*)$ and $B(t) = D_2 f(x^*, u^*)$. Stabilizing (9) may be accomplished by solving

$$\min_{u(\cdot)} \int_0^T z(t)^T Q z(t) + v(t)^T R v(t) \quad dt \tag{10}$$

where Q, R, M are positive definite matrices. The solution to (10) is known to be

$$u_{opt}(t) = R^{-1}B(t)^T P(t) z(t) = K(t)z(t) \tag{11}$$

where P is the solution to the Riccati equation with final condition

$$-\dot{P} = A^T P + PA + Q - PBR^{-1}B^T P$$
$$P(T) = 0$$

This particular feedback design method was chosen for two reasons. First, solving the LQR problem involves selecting matrices Q and R. These matrices balance the cost of the optimization between tracking errors and control perturbations which gives the designer flexibility in the design. Secondly, the optimal control in (11) is guaranteed to stabilize the linearization (9) around the desired trajectory because $V(t, z(t)) = z(t)^T P(t) z(t)$ is a Lyapunov function for (9). The stabilization is valid for some region local to the desired trajectory.

4 Simulation Study

In this section we present results of trajectory morphing on the MLEGM. For this study, a four layer MLEGM was chosen; hence we have 12 states. Showing all of the 12 state trajectories is cumbersome and messy. So, to simplify the presentation, the output of each trajectory of interest will be shown and the relative state and control tracking errors will be shown as a measure of the overall tracking accuracy. Tracking errors will be computed using an L_2 norm.

One complete step of the morph will be presented. Although the morphing process is not shown carried out all the way to $\lambda = 1$, there is no conceptual difference between the first and subsequent morphing steps.

Following the algorithm presented in Section 3, the first step in trajectory morphing is to generate a feedback law that stabilizes a nominal (desired) trajectory. The nominal trajectory was taken to be the one resulting from applying constant controls to the simple model. This was shown in Figure 2. This nominal trajectory was then used to compute the linearization of the MLEGM along this trajectory. The linearization was then used in computing a LQR feedback law described in Section 3.1. The final trajectory tracking feedback controller used for projection was

$$u(t) = \mu(t) + K(t)(\alpha(t) - x(t)) \tag{12}$$

Note that this feedback law satisfies the invariance condition in (6).

The next step in the morphing process is to solve the optimization problem in (7). The homotopy scalar was incremented to a small value, $\lambda = 0.1$. Then the initial guess for a trajectory was projected onto the $\lambda = 0.1$ system trajectories. At this point, the initial guess is simply the nominal trajectory. Figure 3 shows the nominal output and the projected output. Also shown is the state and control tracking errors. A relatively large

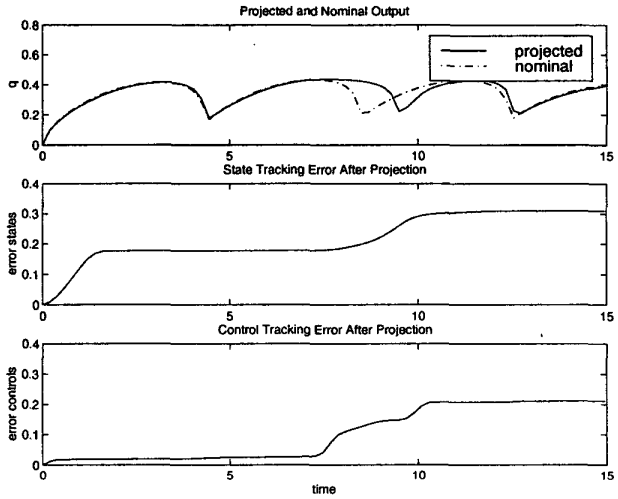

Figure 3: Projected Output and Tracking Errors

deviation in output appears at about 8 seconds into the trajectory. At the same time, there is also a relatively large increase in state and control tracking error. The state-tracking error for the entire trajectory was 0.31 and the control-tracking error was 0.21.

The optimization problem was then solved using a steepest descent method. See [5] for a description. After calculating the steepest descent direction of the functional, a scaled version of the steepest descent was added to the current trajectory guess and then projected onto the system trajectories. The result is the morphed trajectory (again, one step shown). Figure 4 shows the morphed output and its associated tracking errors. As is shown the large deviation in the middle of the output trajectory has been diminished. Although there is noticeable deviations in output tracking at more locations along the trajectory, the overall state-tracking error was reduced from 0.31 to 0.22, a reduction of 29%. The overall control-tracking error also went down slightly from

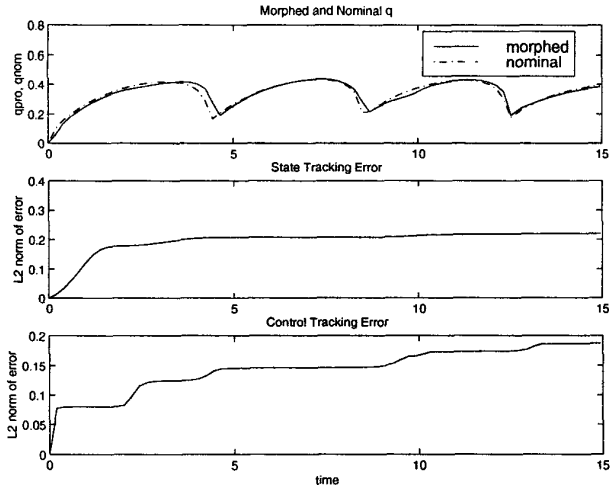

Figure 4: Morphed Output and Tracking Errors

0.21 to 0.19. The final controls that resulted from this step of morphing are shown in Figure 5.

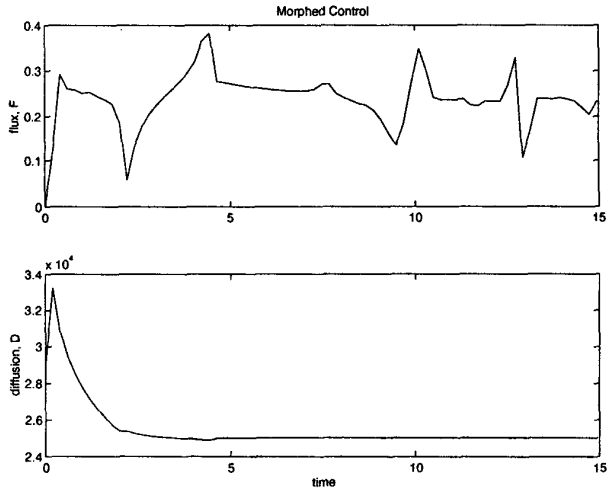

Figure 5: Morphed Controls after Morph Step.

5 Conclusion

In conclusion, it has been shown that trajectory morphing can be successfully applied to explore the trajectory space for an epitaxial thin film growth model. A multi-layer epitaxial thin film growth model was presented along with a simplified version used to generated a desired trajectory for the full model.

References

[1] Bennett, Adam, *Nonlinear Modeling and Control Design for Substrate Temperature in Molecular Beam Epitaxy* , PhD dissertation, University of Colorado, 1998.

[2] Caflisch, R.E., M. Gyure, B. Merriman, S. Osher, C. Ratsch, D. Vvedensky, and J. Zinck. "Island Dynamics and the Level Set Method for Epitaxial Growth", 1998.

[3] Caflisch, R.E., W. E, M. Gyure, B. Merriman, C. Ratsch, "Kinetic Model for a Step Edge in Epitaxial Growth ", 1998.

[4] Caflisch, R.E., M. Gyure, D. G. Meyer, C. Ratsch, "A Reduced Order Model for Epitaxial Growth", 1998.

[5] Hauser, John, Personal notes entitled "Local Optimization of a Trajectory Functional", 1998.

[6] Hauser, John, and David G. Meyer, "Trajectory Morphing for Nonlinear Systems", *Proc. American Control Conference*, Philadelphia, Penn., 1998, ppg 2065-2070.

[7] Hauser, John, and David G. Meyer, "The Trajectory Manifold of a Nonlinear System", *1998 Conference on Decision and Control1*, Tampa, Florida, 1998, ppg 1034-1039.

[8] Jackson, Andrew W., P.R. Pinsukanjana, A.C. Gossard, and L.A. Coldren, "In Situ Monitoring and Control for MBE Growth of Optoelectronic Devices", *IEEE Journal of Selected Topics in Quantum Electronics*, Vol. 3, No. 3, June 1997.

[9] Kailath, T., Linear Systems, Prentice-Hall Inc.,1980.

[10] Tucker, Matthew K., and David G. Meyer, "Nonlinear Modeling, Identification, and Feedback Control Design for the Modern Effusion Cell", *Journal of Vacuum Science and Technology A*, Vol. 16, No. 6., pp. 3536-3553, Nov/Dec 1998.